# MACROSCOPIC COHERENT MAGNETIC ISLANDS

F. Porcelli[1,2], A. Airoldi[3], C. Angioni[4], A. Bruschi[3], P. Buratti[5], F. Califano[6], S. Cirant[3], I. Furno[4], D. Grasso[1], E. Lazzaro[3], A.A. Martynov[4], M. Ottaviani[7], F. Pegoraro[6], G. Ramponi[3], E. Rossi[8], O. Sauter[4], C. Tebaldi[9] and O. Tudisco[5]

[1] INFM and Department of Energetics, Politecnico di Torino, Turin, Italy
[2] Plasma Science and Fusion Center, M.I.T., Cambridge, MA, USA
[3] IFP, Ass. EURATOM-ENEA-CNR, Via Cozzi 53, Milan, Italy
[4] CRPP, Ass. EURATOM-Conf. Suisse, EPFL, Lausanne, Switzerland
[5] Ass. EURATOM-ENEA, Frascati, Italy
[6] INFM and Department of Physics, University of Pisa, Italy
[7] DRFC, CEA Cadarache, 13108 St. Paul lez Durance, France
[8] IFS, University of Texas at Austin, Texas, USA
[9] Department of Mathematics, University of Lecce, Italy

e-mail contact of main author: porcelli@polito.it

**Abstract:** We present experimental and theoretical investigations on the dynamics of coherent magnetic islands in high temperature, magnetically confined plasmas of thermonuclear interest, and of their effects on plasma transport.

## 1. Diamagnetic rotation of magnetic islands

Often, the confinement properties of tokamak plasmas are limited by the onset of macroscopic, coherent magnetic islands. The qualification *coherent* refers to single-helicity islands where chaotic field line behavior does not play an important role. Typically, coherent islands correspond to magnetic perturbations with low poloidal mode numbers, such as neoclassical tearing modes and $m = 1$ resistive kinks. The nonlinear evolution of these islands is still an open problem.

Diamagnetic effects are known to influence significantly the reconnecting magnetic instabilities. The important changes to the classic resistive tearing mode occur in the so called drift-tearing regime [1], when the electron diamagnetic frequency $\omega_{*e}$ is sufficiently larger than the (normalized) growth rate, $\gamma_T = 0.55(\Delta')^{4/5}\eta^{3/5}$, obtained by the RRMHD model, which ignores the equilibrium pressure gradients. For values of $\omega_{*e}/\gamma_T$ exceeding a critical threshold, the eigenfunction undergoes a transition to a radially oscillating, delocalized mode. One can construct an initially localized wavepacket, which propagates outwards undergoing spatial amplification. Furthermore, the nominal mode growth rate, which is obtained from the dispersion relation ignoring the localization problem, is strongly suppressed at high $\omega_{*e}/\gamma_T$. A localized mode can be found when additional physics is included in the models. An important localizing non-dissipative effect, which can lead to the complete stabilization of the drift-tearing mode, is the finite $\beta$ coupling to sound waves [2]. Localization is also achieved by the introduction of appropriate dissipative effects. The roles of two such effects, the ion viscosity and the particle diffusivity, are discussed in this Section.

Diamagnetic effects are altered in the nonlinear regime, as density and temperature profiles tend to flatten, on average, across the island region. This leads to two main questions: (i) To what extent the stabilizing diamagnetic effects are suppressed in the nonlinear saturated regime; (ii) What are the actual mode structure and rotation frequency of saturated islands. These questions are especially relevant when treating more

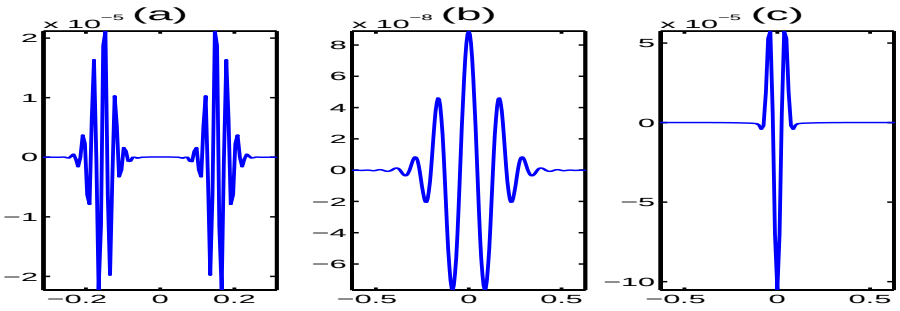


Figure 1: Perturbed current density. (a) Non-localized structure, P=D=0; (b) Viscosity localization, $P = 0.1$, $D = 0$; (c) Diffusivity localization, $D = 0.01\eta$, $P = 0$.

general models that predict full linear stability as in Ref. [2], when one can argue that the nonlinear suppression of the diamagnetic effects could lead to bistability, that is, the coexistence of states with and without magnetic islands for the same set of parameters.

In order to address these issues, we consider the three-field nonlinear version of the model of Ref. [1], with the inclusion of ion viscosity and particle diffusivity. The cold ion limit is taken for simplicity and the electron temperature is constant. The (suitably normalized) vorticity equation is

$$dU/dt = [J, \psi] + \mu \nabla^2 U \tag{1}$$

where $\phi$ is the electric potential, $U = \nabla^2 \phi$ the vorticity, $\psi$ is the magnetic flux function and $J = -\nabla^2 \psi$ is the current density; $[A, B] \equiv (\partial_x A)(\partial_y B) - (\partial_x B)(\partial_y A)$, $d/dt \equiv \partial/\partial t + [\phi, \cdot]$, and $\mu$ is viscosity. The Prandtl number is $P = \mu/\eta$. We adopt the Ohm law

$$d\psi/dt + v_* \partial_y \psi = [n, \psi] - \eta \left( J - J_{eq} \right), \tag{2}$$

where $v_*$ is proportional to the equilibrium density gradient, while the fluctuating density, n, obeys the continuity equation

$$dn/dt + v_* \partial_y \phi = D \nabla^2 n, \tag{3}$$

with $D$ the particle diffusivity. These equations are defined in a box $[-L_x, L_x] \times [-L_y, L_y]$, with aspect ratio $\epsilon = L_x/L_y$ and periodic boundary conditions. The system is driven by the equilibrium current density, $J_{eq}(x) = \cos(x)$ (having set $L_x = \pi$). Following standard techniques, we define the tearing mode stability parameter, $\Delta'$. For the considered equilibrium, $\Delta' = 2\kappa \tan \pi\kappa/2$, where $\kappa = \sqrt{1 - m^2\epsilon^2}$ and $m$ is an integer. Tearing perturbations $\phi = \phi_L(x) e^{ik_y y}$, with $k_y = m\epsilon$, are linearly unstable when $\epsilon < 1$ ($\Delta' > 0$).

The linearized system can be solved analytically. For reason of brevity, we omit the analytic derivation and present only a brief summary of the main interesting regimes.

$\mathbf{P = D = 0}$. The tearing mode growth rate, $\gamma = \gamma_T$, is obtained when also $\omega_{*e} = k_y v_* = 0$. For sufficiently large values of $\omega_{*e}/\gamma_T$, the mode becomes delocalized. Fig. 1a shows an example of what happens to the perturbed current density during the initial growth of the instability for $\eta = 1. \times 10^{-4}$, $\Delta' = 0.71$ and $\omega_{*e}/\gamma_T = 3$.

$\mathbf{P \neq 0}$. For nonzero values of the Prandtl number, a turning point is introduced in space, beyond which the eigenfunction decays exponentially to zero. When $\omega_{*e}/\gamma_T > 1$ and $\mu > \omega_{*e}^{7/3} (\Delta')^{-2/3}$, a new scaling for the growth rate is found, $\gamma \sim \Delta'^{6/5} \eta^{4/5} \omega_{*e}^{-1/5} P^{-1/5}$. An example of the eigenfunction for $P = 0.1$, $\eta = 1. \times 10^{-4}$, $\Delta' = 0.71$ and $\omega_{*e}/\gamma_T = 3$ is shown in Fig. 1b. The mode is now localised with radial oscillations.

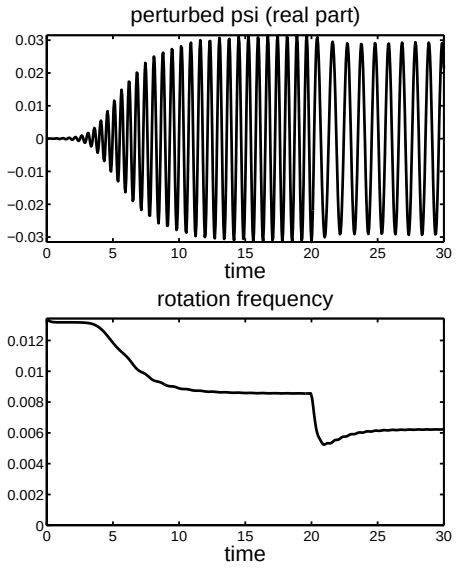


Figure 2: Nonlinear evolution. Top panel: magnetic signal. Bottom panel: rotation frequency.

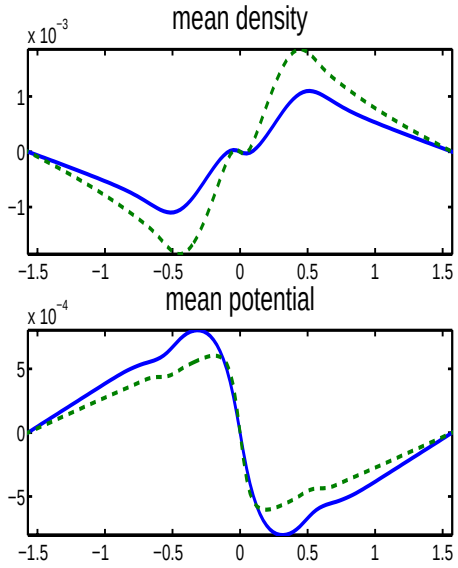


Figure 3: Mean fields, density and potential, for $D = 5. \times 10^{-5}$ (solid) and $D = 2.5 \times 10^{-5}$ (dashed)

**D** $\neq$ **0**. The most striking effect on the mode structure is found for nonzero values of the diffusivity parameter. At $D/\eta \sim 10^{-2}$, the mode structure is localized even for $P = 0$, in addition the radial oscillations are wiped out completely. The effect on the mode growth rate is negligible, as can be shown analytically. An example of the numerical solution is shown in Fig. 1c, for $\eta = 10^{-4}$, $\Delta' = 0.405$, $\omega_{*e}/\gamma_T = 3$ and $D = 5. \times 10^{-6}$.

We also present preliminary nonlinear studies of Eqs. (1)-(3), aimed at identifying the interesting phenomenology. Fig. 2 shows the evolution of the magnetic signal of the dominant mode and the rotation frequency. For this run, $\Delta' = 0.34$, $\eta = 1. \times 10^{-3}$, $P = 0.2$, $D = 5. \times 10^{-5}$ and $\omega_{*e} = 0.015$. The mode initially grows exponentially and rotates at the linear frequency $\omega_{\rm lin} \approx 0.013$, but then it slows down to a somewhat lower frequency. This is accompanied by a reduction of the mean density gradient in the island region. Density flattening is caused by the electric field advection in the continuity Eq. (3) and is counterbalanced by the diffusivity. Fig. 2 also shows that when the diffusivity is reduced to $D = 2.5 \times 10^{-5}$, as we do at time $t = 20$, the frequency further drops. Fig. 3 shows the profiles of the mean fields for two values of diffusivity. We also find that the amplitude of the saturated island is only weakly affected by the diamagnetic frequency, being about 10% less than the amplitude obtained with the RRMHD model for the corresponding value of $\Delta'$.

Neo-classical tearing modes can be destabilized in weakly collisional toroidal plasmas, as a consequence of the local reduction of the bootstrap current within a magnetic island of finite width in an otherwise stable equilibrium with $\Delta' < 0$ [3]. The local current reduction follows the quasi-linear pressure flattening within the island region. While the proposed theoretical models appear to be in qualitative agreement with experimental observations [4], nonlinear diamagnetic effects, which as argued in the previous Section are expected to play an important role, have not been properly included in the models. Furthermore, the critical threshold, in terms of the initial seed island for the onset of these modes, is still an open question [5].

The dynamics of coupled rotating magnetic islands associated with ERCH can be interpreted on the basis of nonlinear model equations, given in detail in Ref. [6], which

describe the interaction of the island inertia with the resistive wall braking torque and the electro-dynamic coupling of the mode side-bands. Coupling can have a stabilizing or destabilizing effect, depending on the phase difference, $\Delta\phi$, which evolves non-linearly in a pendulum-like fashion. During an ECRH pulse in FTU, e.g. shot #14979 shown in Fig. 4 of Ref. [6], the $m/n$ =1/1 and $m/n = 2/1$ magnetic islands initially rotate at a common frequency controlled by the larger of the two islands. This frequency is occasionally seen to jump between the natural frequencies, which, in the plasma rest frame, are related to the electron diamagnetic frequencies at the corresponding mode-rationale surfaces. The frequency jump is the result of the competition between the mutual torques associated with the two islands, viscous drag and wall braking.

## 2. Sawteeth and core plasma transport

Sawtooth crashes are triggered by internal m=1 kink modes [7] when $q < 1$. Non-ideal MHD considerations are necessary in order to understand the actual threshold for the sawtooth crash and the resulting sawtooth period and amplitude. The instability condition can be written as [8] $\delta W < \delta W_{crit}$, where $\delta W = \delta W_{mhd} + \delta W_{KO} + \delta W_{fast}$ is an effective potential energy functional, with $\delta W_{mhd}$ the ideal MHD part [9], $\delta W_{KO}$ the part contributed by the thermal trapped ions [10], $\delta W_{fast}$ the fast particle contribution [11] and $\delta W_{crit}$ is a critical threshold determined by microscopic effects (i.e. electron-ion collisions, ion Larmor radius, electron skin depth, diamagnetic frequency, etc.) in a narrow reconnection layer around the $q = 1$ surface. Detailed expressions for $\delta W$ and $\delta W_{crit}$ can be found in Ref. [8].

Besides fast ions, an important ingredient associated with the stability criterion is the local magnetic shear. For most tokamak discharges of interest today, including TCV and FTU, the relevant layer physics corresponds to the so-called ion-kinetic regime [12], where electron-ion collisions, the ion Larmor radius and diamagnetic effects are important. Under these circumstances, the instability condition is equivalent to $\max(\gamma_\rho, \gamma_\eta) > c_*(\omega_{*e}\omega_{*i})^{1/2}$, where $\gamma_\rho$ and $\gamma_\eta$ are the ion-kinetic and resistive kink growth rates, respectively, $c_*$ is a numerical factor of order unity and the diamagnetic frequencies are evaluated at $r_1$. This condition can be recast in terms of a critical magnetic shear condition for the local parameter $s_1 = r_1 q'(r_1)$. For the case $\gamma_\rho > \gamma_\eta$:

$$s_1 > s_{1,crit} = c_*^{7/6} \left[\pi T_i/2(T_i + T_e)\right]^{1/3} \tau_A^{7/6} (\omega_{*e}\omega_{*i})^{7/12} (r_1/\rho_i)^{2/3} S^{1/6}, \qquad (4)$$

where $\tau_A$ is the relevant Alfven time, $\rho_i$ is the ion Larmor radius and $S$ is the magnetic Reynolds number. A numerical model for sawteeth can be implemented in transport codes, such as PRETOR, based on the following rules. During simulated sawtooth ramps, stability parameters are monitored; when condition (4) is satisfied, a sawtooth crash is triggered, the $q$ profile is relaxed following, for instance, Kadomtsev's full reconnection prescription [7] or a partial reconnection rule, and density and temperature profiles are relaxed accordingly. In this way, repetitive sawteeth can be simulated.

Sensitivity to local magnetic shear was tested in JET discharges with fast wave current drive, where phasing of the ICRH antennas led to lengthening or shortening of the sawtooth period, depending on the sign of the driven current, when the resonant absorption layer was close to the $q = 1$ radius [13]. Similarly, various experiments performed on TCV have highlighted the strong sensitivity of the sawtooth period on ECH and ECCD operation conditions [14]. In Fig. 6, we present a PRETOR sawtooth simulation a dedicated experiment, showing the influence of even small amounts of current drive close to the q = 1 surface [15]. Two shots with identical plasma conditions have been produced: in one case, shot ♯15278, the ECH power is accompanied by CNTR-CD, less than 1% of

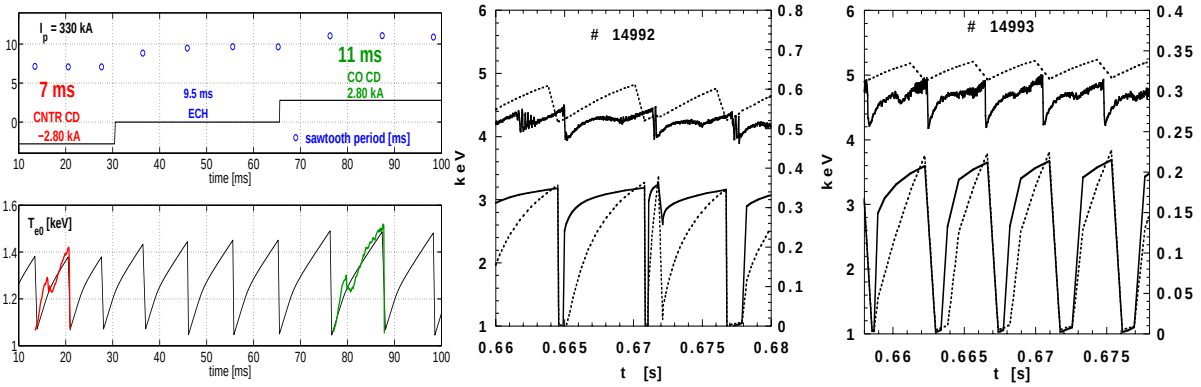


(a) *TCV shots ♯15278 and ♯15282. Top panel: EC current drive as a function of time. Bottom panel: Central electron temperature. Also shown in the bottom panel are two experimental soft x-ray traces.*

(b) *FTU #14992 with co-ECCD applied near $q = 1$. Upper traces: experimental (solid line) and simulated (dotted lines) $T_{e0}$; lower traces: $s_1$ (dotted line) and $s_{1,crit}$ (solid line).*

(c) *FTU #14993 with counter-ECCD applied near $q = 1$. Upper and lower traces: same as in part (b).*

Figure 4: *Sawtooth simulations.*

the plasma current; in the second case, shot ♯15282, the same amount of CO-CD is used. The sawtooth period changes experimentally from 7 to 11 ms. The simulated sawtooth periods reproduce the observed trends. As the ECH power deposition is nearly the same in the two cases, the simulated critical shear as function of time is similar for the two discharges. On the contrary, a small amount of CD, well localized close to the q = 1 surface, changes the evolution of the magnetic shear at q = 1, i.e., $s_1$ increases more quickly after a crash with CNTR-CD and more slowly with CO-CD. Thus, the simulated sawtooth is longer with CO-CD, in very good agreement with the experimental data. FTU sawtooth simulations also show good agreement with experimental results [16], as can be seen in Figs. 4b and 4c.

In a separate development, a numerical code (M1TEV) which solves the thermal energy diffusion equation during localized ECRH heating and the growth of an m/n=1 magnetic island, has been applied to the interpretation of temperature filaments in RTP and TEXT-U and nonstandard sawtooth relaxation oscillations in TCV and FTU, see refs. [17, 19, 18].

## 3. Collisionless magnetic reconnection

Magnetic reconnection in collisionless plasmas was originally motivated by applications to space plasma processes, such as reconnection events occurring in the Earth magneto-tail. Renewed interest in this problem was prompted by the observation of fast sawtooth relaxations in JET. Wesson [20], using a semi-heuristic argument *a la* Sweet-Parker, was the first to point out that electron inertia may give short crash times. More detailed analytic and numerical work [21, 22, 23] showed that: (i) The actual fast reconnection time scale in JET relevant regimes, $\tau_{rec}$, is determined by a combination of the electron skin depth, $d_e$, and the ion (sound) gyroradius, $\rho_s$, namely $\tau_{rec} \sim \tau_A r_1/(d_e \rho_s^2)^{1/3}$, which gives values of $\tau_{rec}$ close to the observed $\tau_{crash} \sim 50 \mu s$ for JET parameters; (ii) The structure of the collisionless reconnection region is very different from that associated with the classic,

collisional Sweet-Parker process.

An appropriate model for collisionless reconnection is Eq. (1), with $\mu = 0$, and the collisionless version of Ohm's law,

$$\frac{\partial F}{\partial t} + [\varphi, F] = \rho_s^2 [U, \psi], \tag{5}$$

where $F = \psi + d_e^2 J$ is the velocity-space-averaged canonical momentum along the ignorable z-direction. The term proportional to $\rho_s^2$ represents electron compressional effects, which are important insofar as $\rho_s > d_e$. Eqs. (1) and (5), together with $U = \nabla^2 \phi$ and $J = -\nabla^2 \psi$, are a closed set. In Refs. [22, 23], these equations were solved in a planar slab subject to double periodic boundary conditions. Choosing a slab aspect ratio $\epsilon = 0.5$ and values of $d_e$ and $\rho_s$ such that $\Delta' d_e > (d_e/\rho_s)^{1/3}$, a quasi-explosive nonlinear growth was found on the time scale $\tau_{rec}$ indicated above, although the adopted boundary conditions limited the interesting nonlinear phase to island widths smaller than the box size (see also Ref. [24]). More recently, we have solved the same set of equations removing the double periodic boundary conditions. We have adopted a Harris pinch equilibrium, $\mathbf{B}_{eq} = B_0 \mathbf{e}_z + B_{yeq}(x) \mathbf{e}_y$, where $B_{yeq}(x) = \tanh(x/L)$ and $L$ is the equilibrium scale length. This equilibrium is unstable to tearing perturbations, periodic in $y$ over the distance $L_y$, when $L < \pi L_y$. In the $x$ direction, we impose the fields $\phi$ and $\psi - \psi_{eq}$ to vanish at infinity. The linear (small perturbation) phase can be solved analytically. In the limit $\Delta' \to \infty$, the linear growth rate [21] $\gamma_L \tau_A \approx (2 d_e \rho_s^2/\pi)^{1/3}/r_1$ is recovered. With the Harris-pinch configuration, a single coherent magnetic island can be followed in time, until its width saturates at a macroscopic amplitude. Numerical results confirm that the magnetic island grows to a macroscopic amplitude in a quasi-explosive manner and approaches saturation on the time scale $\tau_{rec} \sim \gamma_L^{-1}$.

The collisionless model we have adopted admits two families of topologically invariant fields:

$$G_\pm = F \pm d_e \varrho_s U. \tag{6}$$

Equations (1) and (5) can be written as

$$\frac{\partial G_\pm}{\partial t} + [\varphi_\pm, G_\pm] = 0, \tag{7}$$

where $\varphi_\pm = \varphi \pm (\varrho_s/d_e)\psi$. The energy functional playing the role of the system Hamiltonian [25] is $H = -(1/2) \int d^2x (\varphi_+ G_+ + \varphi_- G_-)$. Eq. (7) expresses the Lagrangian conservation of the fields $G_\pm$, advected by the generalized flows $\mathbf{v}_\pm = \mathbf{e}_z \times \nabla \varphi_\pm$. Clearly, any function of $G_\pm$ is also a conserved field. We have shown in Ref. [23] that the existence of these topological invariants is responsible for the structure of the reconnection region, in particular the cross-shaped structure of the current density and vorticity layers and the generation of microscales below the electron skin depth. A more general question of principle that we address here is how to reconcile the reversible energy transport to small scales implied by the dissipationless evolution, with the seemingly irreversible approach to a saturated equilibrium with a macroscopic magnetic island.

The resolution of this apparent paradox [26] is spatial phase mixing of the Lagrangian invariants, i.e. the functions $G_\pm$ develop fine scale oscillations as they are advected by vortical patterns corresponding to the velocity fields $\mathbf{v}_\pm$, while the functions $\phi$ and $\psi$, that can be expressed through integrals of $G_\pm$, turn out to be smooth. This process can be more easily understood in terms of a formal analogy with the standard Vlasov-Poisson problem for electrostatic Langmuir waves. The set of Eqs. (7) has the form of two coupled 1D Vlasov equations, with $x$ and $y$ playing the role of the coordinate and the conjugate

momentum for the "distribution functions" $G_\pm$ of two "particle" species with equal charges in the Poisson-like equation, $d_e\rho_s\nabla^2\phi = (G_+ - G_-)/2$, and opposite charges in the Yukawa-type equation, $\psi - d_e^2\nabla^2\psi = (G_+ + G_-)/2$. The generalized stream functions $\phi_\pm$ play the role of the single particle Hamiltonians. Thus, similarly to Bernstein-Green-Kruskal [27] solutions, the stationary solutions can be written in the form $G_\pm = \mathcal{G}(\phi_\pm)$ (there is a single function $\mathcal{G}$ because of the symmetry relation $G_+(-x, y) = G_-(x, y)$). However, the present problem and the standard Vlasov-Poisson problem are not formally identical. In Poisson's equation, the source term is the electron density, which is the velocity space integral of the distribution function and as such does not exhibit fine scale oscillations. In our problem, the source terms for the Poisson-type and Yukawa-type equations are the distribution functions $G_\pm$ themselves. On the other hand, the fields $\phi$ and $\psi$ solutions of these equations can be expressed in terms of integrals of $G_\pm$. Therefore, the fine scale structure of $G_\pm$ does not show up in $\phi$ and $\psi$. We conclude that phase mixing of the Lagrangian invariants can allow the plasma to access a new "macroscopic" stationary state, similar to the formation of macroscopic BGK equilibria [27], without violating energy conservation. Indeed, separating the Lagrangian invariants into coarse-grained and phase-mixed parts, the latter are contributed by small scale filaments and have zero space average. Therefore, one finds the contributions of the phase-mixed parts of $\psi$ and $\varphi$ to be negligibly small, as $\psi$ and $\varphi$ are obtained from $G_\pm$ upon spatial integration. On the other hand, these small scale structures continue to contribute to total energy conservation through the quadratic $d_e^2 J^2$ and $\varrho_s^2 U^2$ terms in the energy integral $H$.

## 4. Conclusions

We have presented recent advances on the understanding of macroscopic island dynamics in magnetized plasmas, made possible by a profitable interaction between theory and experiments. The understanding, however, is still incomplete. The main conclusions to date can be summarized as follows:
1) A satisfactory model for the sawtooth period and amplitude has been developed and validated against TCV and FTU experiments. The model points to the importance of diamagnetic effects, which introduce a threshold for the trigger of the sawtooth crash in terms of a critical value of the local magnetic shear parameter. Localized current drive can influence the time evolution of the local magnetic shear and thus represents an effective means for sawtooth control. The model also includes the stabilizing effects of fast ions. Thus, the proposed sawtooth model is a state-of-the-art viable tool for predicting sawtooth behavior in future experiments, and as such it has been implemented in predictive transport codes such as PRETOR.
2) Diamagnetic effects are important also for the dynamics of nonlinear (neoclassical) tearing modes, which in FTU are observed rotating at the electron diamagnetic frequency. A nonlinear model for the dynamics of coupled rotating islands has been developed and compared with FTU data. In another theoretical development, preliminary results on the evolution of nonlinear drift-tearing modes, based on a reduced three field model, have been presented. It is shown that density gradients in the reconnection region can be maintained nonlinearly and give rise to island diamagnetic rotation.
3) A model for the evolution of electron temperature profiles during sawteeth and localized ECRH has been developed and compared against TCV and FTU data.
4) In large size tokamaks such as JET, sawtooth reconnection can occur under nearly collisionless conditions. We have shown that nonlinear collisionless reconnection is fast enough to account for the observed sawtooth crash time in JET. As a matter of principle, we have also shown that growth and saturation of magnetic islands can occur in collision-

less conditions. Irreversibility in collisionless reconnection is introduced by spatial phase mixing of conserved fields. In this sense, magnetic island saturation has a formal analogy with the formation of BGK equilibria for dissipationless Langmuir waves.

# References


[1] ARA,G., et al., Ann. Phys. 112 (1978) 443.

[2] BUSSAC, M.N., et al., Phys. Rev. Lett. 40 (1978) 1500.

[3] HEGNA, C.C., CALLEN, J.D., Phys. Fluids B 4 (1992) 4072.

[4] SAUTER, O., et al., Phys. Plasmas 4 (1997) 1654.

[5] WAELBROECK, F.L., FITZPATRICK, R., Phys. Rev. Lett. 78 (1997) 1703.

[6] LAZZARO, E. , et al., Phys. Rev. Lett. 84 (2000) 6038.

[7] KADOMSTEV, B.B., Fiz. Plasmy 1 (1975) 710; Sov. J. Plasma Phys. 1 (1975) 389.

[8] PORCELLI, F., et al., Plasma Phys. Contr. Fusion 38 (1996) 2163.

[9] BUSSAC, M.N., et al., Phys. Rev. Lett. 35 (1975) 1638

[10] FOGACCIA, G., ROMANELLI, F. Phys. Plasmas 2 (1995) 227.

[11] PORCELLI, F. Plasma Phys. Contr. Fusion 33 (1991) 1601.

[12] PEGORARO, F., et al., Phys. Fluids B 1 (1989) 364.

[13] BHATNAGAR, V.P., Nucl. Fusion 34 (1994) 1579.

[14] GOODMAN, T.P., et al., proc. 26th EPS Conf. Maastricht, 1999.

[15] ANGIONI, C., et al., to be published in *Theory of Fusion Plasmas*, Proc. Joint Varenna-Lausanne Int. Workshop, Varenna, 2000.

[16] RAMPONI, G., et al., in Proc.of 13th Top. Conf. on Radio Frequency Power in Plasmas, Annapolis 1999, AIP Conf. Proc. Vol.485, p.265.

[17] PORCELLI, F. et al., Phys. Rev. Lett. 82 (1999) 1458.

[18] FURNO, I., et al., CRPP Report LRP 665/00, May 2000, submitted to Nuclear Fusion.

[19] PORCELLI, F. , et al., Nuclear Fusion to appear (Oct 2000 issue).

[20] WESSON, J., Nucl. Fusion 30, (1990) 2545.

[21] PORCELLI, F., Phys. Rev. Lett. 66, (1991) 425.

[22] OTTAVIANI, M., PORCELLI, F., Phys. Rev. Lett. 71 (23), (1993) 3802.

[23] CAFARO, E., et al., Phys. Rev. Lett. 80 (1998) 20.

[24] LAZZARO, E., et al., Phys. Scripta 61 (2000) 624.

[25] KUVSHINOV, B.N., et al., Journ. Plasma Phys. 59 (1998) 4.

[26] GRASSO, D., et al., submitted to Phys. Rev. Lett. (2000).

[27] BERNSTEIN, I.B., et al., Phys. Rev. Lett. 108 (1957) 546.